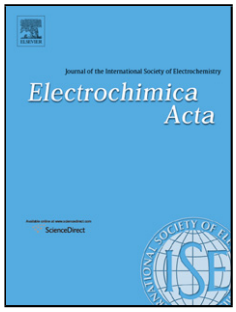

Title: PERFORMANCE ASSESMENT OF A POLYMER ELECTROLYTE MEMBRANE ELECTROCHEMICAL REACTOR UNDER ALKALINE CONDITIONS – A CASE STUDY WITH THE ELECTROOXIDATION OF ALCOHOLS

Author: Leticia García-Cruz Clara Casado-Coterillo Ángel Irabien Vicente Montiel Jesus Iniesta

PII: S0013-4686(16)30947-1
DOI: http://dx.doi.org/doi:10.1016/j.electacta.2016.04.110
Reference: EA 27145

To appear in: *Electrochimica Acta*

Received date: 27-1-2016
Revised date: 29-3-2016
Accepted date: 20-4-2016

Please cite this article as: Leticia García-Cruz, Clara Casado-Coterillo, Ángel Irabien, Vicente Montiel, Jesus Iniesta, PERFORMANCE ASSESMENT OF A POLYMER ELECTROLYTE MEMBRANE ELECTROCHEMICAL REACTOR UNDER ALKALINE CONDITIONS *minus* A CASE STUDY WITH THE ELECTROOXIDATION OF ALCOHOLS, Electrochimica Acta http://dx.doi.org/10.1016/j.electacta.2016.04.110

PERFORMANCE ASSESMENT OF A POLYMER ELECTROLYTE MEMBRANE ELECTROCHEMICAL REACTOR UNDER ALKALINE CONDITIONS - A CASE STUDY WITH THE ELECTROOXIDATION OF ALCOHOLS

Leticia García-Cruz[1], Clara Casado-Coterillo[3], Ángel Irabien[3],

Vicente. Montiel[1,2], Jesus Iniesta[1,2 *]

[1] *Institute of Electrochemistry, University of Alicante, 03080, Alicante, Spain*

[2] *Department, of Physical Chemistry, University of Alicante 03080 Alicante, Spain*

[3] *Department of Chemical and Biomolecular Engineering, University of Cantabria, 39005 Santander, Spain.*

*Corresponding author´s email: jesus.iniesta@ua.es

Phone number: +34 965909850

FAX number: +34 965903537

Graphical Abstract

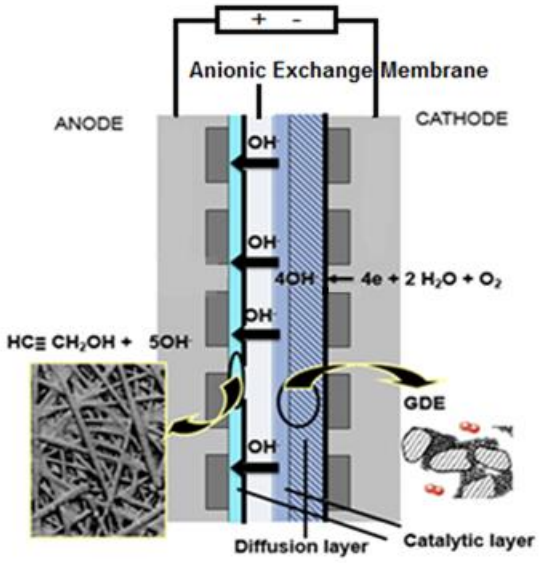

Figure abstract

Abstract

A novel polymer electrolyte membrane electrochemical reactor (PEMER) configuration has been employed for the direct electrooxidation of propargyl alcohol (PGA), a model primary alcohol, towards its carboxylic acid derivatives in alkaline medium. The PEMER configuration comprised of an anode and cathode based on nano-particulate Ni and Pt electrocatalysts, respectively, supported on carbonaceous substrates. The electrooxidation of PGA was performed in 1.0 M NaOH, where a cathode based on a gas diffusion electrode was manufactured for the reduction of oxygen in alkaline conditions. The performance of a novel alkaline anion-exchange membrane based on Chitosan (CS) and Poly(vinyl) alcohol (PVA) in a 50:50 composition ratio doped with a 5 wt.% of poly (4-vinylpyridine) organic ionomer cross-linked, methyl chloride quaternary salt resin (4VP) was assessed as solid polymer electrolyte. The influence of 4VP anionic ionomer loading of 7, 12 and 20 wt.% incorporated into the electrocatalytic layers was examined by SEM and cyclic voltammetry (CV) upon the optimisation of the electroactive area, the mechanical stability and cohesion of the catalytic ink onto the carbonaceous substrate for both electrodes. The performance of the 4VP/CS:PVA membrane was compared with the commercial alkaline anion-exchange membrane FAA –a membrane generally used in alkaline fuel cells- in terms of polarisation plots in alkaline conditions. Furthermore, preparative electrolyses of the electrooxidation of PGA was performed under alkaline conditions of 1 M NaOH at constant current density of 20 mA cm^{-2} using a PEMER configuration to provide proof of the principle of the feasibility of the electrooxidation of other alcohols in alkaline media. PGA conversion to Z isomers of 3-(2-propynoxy)-2-propenoic acid (Z-PPA) was circa 0.77, with average current efficiency of 0.32. Alkaline stability of the membranes within the PEMER configuration was finally evaluated after the electrooxidation of PGA.

Keywords: Polymer Electrolyte Membrane Electrochemical Reactor (PEMER) configuration.PEMER configuration, Anionic alkaline exchange membrane, Anionic ionomer, Chitosan/poly vinyl alcohol membrane, alcohol electrooxidation.

1. Introduction

The use of the electrochemical technology in organic synthetic processes to obtain high value-added products is a relevant alternative against conventional chemical procedures in terms of a more environmentally friendly technology [1, 2]. The development of solid polymer electrolyte (SPE) technology [3], and more specifically, direct alcohol fuel cells applications [4] has been introduced into the field of organic electrosynthesis. In this regard, the concept of Polymer Electrolyte Membrane Electrochemical Reactor (PEMER) has been recently introduced in organic electrosynthesis, e.g. for the N-acetyl-L-cysteine production from the electroreduction of N,N-diacetyl-L-cysteine [5] and the synthesis of 1-phenylethanol from the electroreduction of acetophenone [6, 7] under acidic conditions. Moreover, pioneering work performed by Ogumi and co-workers on the electrochemical hydrogenation of olefinic double bonds [8] and the reduction of nitrobenzene [9] was performed using a Nafion membrane-based SPE, within a similar configuration to PEMER, in which the product purification operations were then reduced. To the best of our knowledge and from a synthetic point of view, there are few works dealing with the electrooxidation of alcohols within a configuration similar to PEMER and/or filter-press electrochemical cell under alkaline conditions [10-12]. Benefits from the electrooxidation of alcohols in alkaline media is based on the more favourable electroorganic process, e.g., the electrooxidation of primary alcohols to its carboxylic acids requires lower anode potentials with a lower cost of electrocatalysts [13, 14].

A PEMER configuration has similar structure to a polymer electrolyte membrane (PEM) fuel cell manufacture, and its manufacture involves the design and preparation of nanoparticulated electrocatalysts as well as gas diffusion layers deposited onto carbonaceous structures, prompting the use of lower metallic electrocatalysts loading. In a PEMER configuration, the supported electrolyte is the SPE, which allows exchange of cations or anions according to the membrane composition. The introduction of SPE allows solving one of the main problems of traditional organic electrosynthesis performed in conventional flow cell and founded on the need for incorporating a supporting electrolyte, which can hinder the subsequent operations such as separation and purification of products. In SPE based electrosynthesis, pure organic liquids or gases (by using a gas diffusion electrode, GDE) can react on the SPEs containing electrodes. In addition, the use of SPE

facilitates the concentration increase of organic reagents and also high working current densities. More importantly, the use of SPE reduces the ohmic drops within an electrolysis cell and increases the mass transport from and to the working electrode by an electro-osmotic flow effect.

Recently, significant efforts are being focused on the production and characterisation of new alkaline anion exchange membranes (AAEMs) as alternative to acidic media, and the commonly used cationic membrane as SPE in a fuel cell [15, 16] or direct alcohol fuel cells [17], to mention only a few examples. The use of AAEMs in alkaline media mainly benefits from the kinetic enhancement of the electrochemical oxygen reduction reaction (ORR); the organic fuels oxidation being favoured at alkaline pH; the utilisation of non-noble metals as electrode materials and the use of membranes without perfluorinated ionomers. Nevertheless, alkaline media also present disadvantages regarding the chemical and mechanical stability of membranes when they are submitted to strong alkaline conditions and elevated temperatures, and the progressive carbonation due mainly to CO_2 coming from atmospheric air or organic fuel oxidation [15]. Thus, AAEMs are vital elements that govern the highest electrochemical performance of a fuel cell or a PEMER, the latter from an electrosynthetic viewpoint. A vast body of literature focuses on the synthesis and characterisation of novel AAEMs or hydroxide exchange membranes (HEMs) with different eco-friendly polymers as continuous matrix such as chitosan [18], and poly(vinyl) alcohol [19], doped with fillers of different nature [20] and cross-linker [21], to adapt the polymers with low electrical resistance, high thermal, mechanical and chemical stability, as well as high permselectivity to PEMER type configuration requirements.

The membrane is not the only limiting element in the performance of a PEM electrochemical reactor, but also the electrocatalytic layers attached to the membrane and the gas diffusion layers. This configuration is called Membrane Electrode Assembly (MEA) and comprises the layers of electrocatalytic materials and membrane intimately bound. With regard to electrocatalytic layer, the functions of the ionomer are (i) binding of nano-particulate electrocatalyst to form a 3D structure facilitating the mobility and transfer of OH^- as well as reactants and products, (ii) increase of electrochemically active surface area (EASA) and (iii) the enhancement of the MEA mechanical durability [17, 22, 23].

Consequently, the ionomer nature and its composition within electrocatalytic layer play a crucial role during the electrochemical processes occurring inside the electrochemical reactor.

This article aims at the manufacture and performance improvement of a 25 cm^2 PEMER configuration, working at controlled current in alkaline media for the electrooxidation of a model alcohol molecule, propargyl alcohol (PGA), toward the synthesis of its carboxylic acid derivatives with interest in industry. In our previous works, we have demonstrated that the electrooxidation of PGA at room temperature leads to the selective formation of Z isomers of 3-(2-propynoxy)-2-propenoic acid (Z-PPA) and propiolic acid (PA) [14, 24] using an electrochemical H-cell type. Both Z-PPA and PA compounds are used as (i) polishing agents in electroplating baths to improve metal deposition, (ii) corrosion inhibitors and (iii) intermediates in organic syntheses [25]. For the scale-up of the electrosynthesis process, we have for the first time developed, manufactured, and characterised the three main parts of a PEMER configuration: a nickel based nanoparticulated anode for the electrooxidation of our model alcohol PGA, a platinum based nanoparticulated cathode for the electrochemical ORR, and the AAEM as a SPE separator. X-ray diffraction (XRD) has been used for the determination of crystallite size of the cast films electrocatalysts. Field emission scanning electron microscopy (FESEM) has been used for exploration of topographical and surface microstructure. Moreover, surface elemental analysis and distribution of cast-films has been evaluated using energy-dispersive X-ray spectroscopy. Alternatively, Raman spectroscopy has been also used for the characterization of the electrodes cast films. Cyclic voltammetry (CV) have been also used for the characterisation of the anode and cathode electrodes as a function of the ionomer concentration. After the assembly of the PEMER, PGA conversion and current efficiency towards the two possible final products expected, PA or Z-PPA have been explored for several consecutive electrolysis.

As alternative membranes to commercial AAEMs, our recent research has demonstrated that membranes based on chitosan (CS) and polyvinyl alcohol (PVA) doped with organic ionomers and layered inorganic fillers exhibit good mechanical properties, thermal and chemical stability, with an improvement of conductivities and reduced alcohol permeability in direct alcohol oxidation in a PEMER configuration [26]. Interestingly, the use of the

poly (4-vinylpyridine) cross-linked, methyl chloride quaternary salt resin ionomer binder (4VP), which is employed in numerous works dealing with alkaline fuel cells [27-30], has provided excellent performance for the CS:PVA polymeric blend membrane (4VP/CS:PVA) in terms of ionic conductivity with values over 1.0 mS cm^{-1}. Hence, as an alternative to the commercial AAEMs, this work aims also to look into for the first time the feasibility of less expensive and biodegradable 4VP/CS:PVA membrane for the electrooxidation of alcohols in alkaline medium using a PEMER configuration. Hence, the overall goal of this manuscript relies on the feasibility to scale-up the electrochemical oxidation of primary and secondary alcohols as described in our patent [31] with higher performances compared to conventional electrochemical procedures.

2. Experimental

2.1 Chemicals and reagents

Propargyl alcohol (PGA) and propiolic acid (PA) were of analytical grade (+ 99% purity, from Alfa Aesar). PGA was purified through distillation before use and its purity was determined by ^{1}H NMR. Vulcan XC-72® carbon powder was purchased from Cabot Corporation (CAS No 1333-86-4, sample number GP 3621). Measured Brunauer-Emmer-Teller (BET) surface area of Vulcan XC-72® is well-established in the literature [32, 33] with a value ca. of 250-300 $m^2 g^{-1}$, and with particle sizes varying between 50 and 60 nm. The ion exchange cross-linked, Poly (4-vinylpyridine) cross-linked, methyl chloride quaternary salt (4VP) (Molecular Weight: 105.10 g mol^{-1}, CAS:125200-80-8) beads 300-1000 μm particle size and whose molecular structure is represented in Scheme 1, and polytetrafluoroethylene (PTFE) preparation 60 wt % dispersion in water (CAS:9002-84-0) were purchased from Sigma Aldrich. Commercial FAA-3-PEEK-130 anion-exchange membrane was purchased from Fumatech GmbH. The ion exchange cross-linked, methyl chloride quaternary poly (4-vinylpyridine) (4VP) salt resin, whose molecular structure is represented in Scheme 1, and polytetrafluoroethylene PTFE were purchased from Sigma Aldrich. Commercial FAA-3-PEEK-130 anion-exchange membrane was purchased from Fumatech GmbH. The synthesis and characterization of the 4VP/CS:PVA membrane have been described in detail elsewhere[26]. Nickel precursor was a salt of Ni (II) chloride hexahydrate assay 98 % GPR Rectapur from VWR. Ethanol absolute PA-ACS-ISO (99.8

%) was purchased from Panreac. NaOH was purchased of analytical grade (+99 %, from Merck). Pt precursor was a salt of chloroplatinic acid hexahydrate (H_2PtCl_4) ACS Reagent, ≥37.50 % Pt basis from Sigma Aldrich. Sodium citrate tribasic dehydrate, ACS reagent ≥99.0 %, and $NaBH_4$ of analytical grade 99 % purity, were purchased from Sigma Aldrich. All other chemicals were purchased from the highest analytical grade available and were used as received without any further purification. All solutions were prepared using doubly distilled water with a resistivity not less than 18.2 MΩ cm.

2.2 Catalytic inks and electrode preparation

Anode and cathode electrodes were prepared by airbrushing technique. The catalytic inks of the anode and the cathode were sprayed onto a 5 x 5 cm^2 Toray paper (T, TGPH-120) placed on a hot metallic plate at 90 ºC to facilitate solvent evaporation, achieving Ni loading of 0.1 mg cm^{-2} and Pt loading of 1.0 mg cm^{-2}, respectively. The EASA of each electrode was 336.8 m^2 g^{-1} for Ni and 129.3 m^2 g^{-1} for Pt. Such EASA values were calculated by taking into account the loading weight of Ni and Pt and the average nanoparticles spherical size of around 2 nm of average particle size as depicted by TEM images in [24, 34], by assuming that all nanoparticles are equally active or available for their corresponding electrochemical processes.

The anodic ink consisted of an alcoholic dispersion of nickel nanoparticles supported onto carbon black Vulcan XC-72R (Ni/CB) with 20 wt. % metal content in 20 wt. % 4VP ionomer (from a 1.96 wt. % 4VP aqueous solution as mother dispersion) with respect to the total sum of weight of Ni/CB and 4VP. Ni/CB was prepared according to experimental procedure described in previous work [24], in which nickel nanoparticles were synthesised by reducing a 0.1 M $NiCl_2 \cdot H_2O$ salt ethanolic solution salt with $NaBH_4$ in ethanolic sodium hydroxide medium at room temperature under vigorous magnetic stirring with a 1:2:10 weight percentage of Ni(II): $NaBH_4$:NaOH. Ni nanoparticles were thoroughly rinsed with acetone, and then dispersed using an ethanol solution giving rise to a final concentration of ca. 2.6 mg Ni per mL of solution. For the preparation of the Ni/carbon black (NiCB) anode, nickel nanoparticles within an ethanolic suspension were mixed with carbon black powder in adequate amounts to reach nickel loadings of ca. 20 wt.%, and thereafter dispersed for 90 minutes under sonication (Selecta ultrasonic bath operating at

50/ 60 kHz, 360 W power output). Finally, 4VP ionomer in a certain amount to get a specific wt. % value was added into the Ni/CB mixture and then sonicated for 45 minutes.

The gas diffusion electrode (GDE) of the cathode consisted of an electrocatalytic layer made of platinum nanoparticles supported on carbon black (Pt/CB) over a backing layer (a Vulcan XC-72^{R} carbon to PTFE ratio of 40/60 w/w, and Vulcan XC-72 loading of 2.0 mg cm^{-2}), which was supported on a Toray Paper TGPH-120 containing 20 wt. % teflon. The catalytic ink of the cathode was a Pt/CB powder formed by 7, 12 and 20 wt. % of 4VP ionomer (from a 1.96 wt. % 4VP aqueous solution as mother dispersion).

The Pt/CB mixture were prepared according to experimental procedures described Lopez-Cudero et al. [34]. Briefly, an equivalent H_2PtCl_4 and sodium citrate solution was reduced by ice-cold sodium borohydride solution. Then, a certain amount of Vulcan carbon was added until a final 20 wt. % of Pt content. Finally, sodium hydroxide pellets were added to precipitated Pt nanoparticles, which are thereafter filtered through nylon membrane filter of 45 µm (Cat No. MNY045047H, chm by CHMLAB GROUP) and then dried overnight at 70 ºC. The anode and cathode were named as follows: 4VP-Ni/CB/T for the anode and 4VP(z)-Pt/CB/GDE/T for the cathode, where z stands for the wt. % of anionic ionomer and T indicates the Toray paper support.

2.3 Electrodes characterisation

Scanning electron microscopy (SEM, HITACHI S-3000N microscope working at 20 kV with X-ray detector Bruker Xflash 3001 for microanalysis.) was employed to analyse the morphology of the electrocatalytic layers of the manufactured electrodes. High resolution SEM images were obtained using a field emission scanning electron microscopy (ZEISS model Merlin VP Compact.). X Pert PRO MPD diffractometer operating at 45 kV and 40 mA, equipped with a germanium Johansson monochromator that provides Cu Kα1 radiation (λ = 1.5406 Å), and a PIXcel solid angle detector, at a step of 0.05º per min. Electrodes cast films were examined at 25 ºC by powder X-ray diffraction Bruker D8-Advance with mirror Goebel (non-planar samples) with a generator of x-ray KRISTALLOFLEX K 760-80F (power: 3000 W, voltage: 20-60 KV and current: 5-80 mA) with a tube of RX in the wave length 1.5406 – 1.54439 Å. Raman spectrum was recorded

by using LabRam (Jobin-Ivon) with a confocal microscope (x100 objective) spectrometer with a He/Ne laser at 632.78 nm excitation.

The electrochemical characterisation of the different electrocatalytic layers was performed in a three-electrode configuration glass cell, using as underlying electrode a polished glassy carbon (GC) surface or a Toray paper where the catalytic inks for the anode and cathode were deposited by dripping or airbrushing techniques, respectively. A gold wire was used as counter electrode and a AgCl/Ag/ (3.5 M KCl) electrode as reference electrode. Solutions consisted of 1.0 or 0.1 M NaOH and were deoxygenated under argon atmosphere. CV experiments were performed using an Autolab III potentiostat/galvanostat (Eco-Chemie). All Ni based anodes were previously pre-treated between -0.5 and +0.6 V versus the AgCl/Ag/ (3.5 M KCl) reference electrode for 100 cycles at a scan rate of 100 mV s^{-1} to obtain the catalytic form of NiOOH species [14, 24, 35, 36] responsible for catalysing the electrooxidation of alcohols. All CV measurements were performed at 25 ± 1 ºC. Currents CV plots were normalised by the Ni/C or Pt/C loading in milligrams.

2.4 Preparative electrosynthesis

Preparative electrooxidation of PGA was performed using PEMER configuration with a commercial flow distributor based on two graphite plates [7]. The graphite plates consisted of a 25 cm^2 PEM fuel cell hardware, column flow pattern (FC-25-01-DM model, attached with fittings, current collectors, gaskets, banana plugs manufactured by ElectroChem, Inc. Figure 1 shows a scheme of the PEMER configuration. The MEA resulted in a 25 cm^2 projected area. FAA and 4VP/CS:PVA membranes were activated in 1.0 M NaOH for 24 h prior to the experiments and then rinsed, stabilised and stored in deionised water at room temperature. Membranes were placed between the cathode and anode and then the MEA configuration was pressed and assembled between two graphitic column plates that act as anodic and cathodic current collectors. The electrochemical reactor consisted of 4VP-Ni/CB/T as anode and a gas diffusion electrode 4VP(12)-Pt/CB/GDE/T as cathode, both electrodes with a projected area of 25 cm^2. A peristaltic pump (Ismatel Reglo DIG MS/CA 2–8C) provided a controlled flow rate of the anodic solution that was set at 12 mL min^{-1}. The cathode was fed with 50 mL min^{-1} of synthetic air (99.999 % purity from Air Liquid, Spain) and humidified through a distilled water column

at atmospheric pressure controlled by a digital mass flow rate controller (Smart-trak 2 Sierra Intruments, Inc.) before passing through the cathodic compartment. Current, charge passed and cell potential during the electrosynthesis were controlled and monitored using a Gw instek PSP-2010 power supply as current source. Before starting the electrooxidation of PGA, Ni/CB electrocatalytic layer was activated. To do this, the anode compartment was fed with a 1.0 M NaOH solution and then a current was set to 0.3 A for 16 min to obtain the electrocatalytic NiOOH species. Later, polarisation plots were taken at varying current between 0.020 and 0.500 A, where the current was held for 1 min before recording the cell potential. PGA electrooxidation was carried out at room temperature with a controlled current of 0.5 A, i.e., 20 mA cm^{-2} and a charge passed of 2895 C.

For the electrolysis experiments, PGA conversion and the formation of the final products were followed by HPLC, according to the experimental procedure described elsewhere [24]. Electrochemical conversion is defined as the mole ratio between the amount of reactant consumed and the initial amount of reactant for a determined charge passed [37]. As the global rate of an electrochemical reaction can be expressed as a function of electrolysis Faraday law, the amount of reactant consumed represents an equivalent amount of electrical charge involved in electrooxidation process [38]. Current efficiency is defined as the ratio between the charge passed used to form the product and the total charge passed for the electrooxidation of PGA.The final products were confirmed by ^{1}H NMR at 400 MHz with a BRUKER AV300 Oxford instrument. For the final workup of the electrooxidative reaction, liquid–liquid extraction of the acidified final anolyte solution was performed in ethyl ether; thereafter the solvent was dried in anhydrous sodium sulphate and finally concentrated *in vacuum* at 40 ºC.

3. Results and discussion

3.1. Physicochemical and electrochemical characterisation of the Pt/CB/GDE/T cathode

We first investigated the influence of the 4VP anionic ionomer concentration on the electrochemical response of platinum nanoparticles (PtNPs) in 0.1 M NaOH aqueous solution. Figure 2a shows the typical response of PtNPs in this medium [39]. Briefly, the peaks of the voltammogram in the potential range between -0.90 and -0.55 V contains the contributions of hydrogen adsorption/desorption. On the other hand, the potential range

between -0.35 V and 0.0 V shows the characteristic OH adsorption/desorption region. Therefore, an increase of the 4VP ionomer concentration within the Pt/CB ink preparation leads to the blockage or fouling of the Pt surface. Nonetheless, a key point of this work come up about the counterbalance between the electrocatalytic properties of the PtNPs for the ORR and the adequate catalytic ink formulations to enhancing particles cohesion and therefore the formation of a three dimensional structure. With the aim of shedding light on how the 4VP affects the CV pattern of PtNPs, Figure 2b shows the CVs of Pt/CB varying 4VP wt.% of the ink drop-casted onto the polished glassy carbon electrode surface in 0.1 M NaOH. The 4VP content with respect to Pt/CB is examined within a range of 7-20 wt. %. In the absence of 4VP, the CV of Pt/CB nanoparticles depicts well defined the peaks associated with the adsorption/desorption regions of hydrogen and OH [39, 40]. However, the higher the 4VP wt. %, the larger the anionic ionomer adsorption and the blockage of the catalytic surface of the PtNPs, with a consequent reduction of the electroactive area. Hence, a remarkable charge reduction, associated with adsorption/desorption of hydrogen, occurs when 7 wt. % 4VP ionomer are added for the same loading of Pt within the Pt/CB nanoparticles. Not surprising is the fact that an increase in 4VP wt. % from 7 to 12 wt. % is detrimental for the observation of a clear CV pattern of the Pt/CB nanoparticles in alkaline medium. Moreover, the charge involved on the hydrogen and OH adsorption/desorption in the CV of Figure 2b is similar for both 12 and 20 wt. % 4VP.

A comparable behaviour is shown in Figure 2c when we assessed the CV response of the cathodic 4VP(z)-Pt/CB/GDE/T electrode, where the Pt catalytic inks have been sprayed onto the carbonaceous gas diffusion layer supported on Toray. In this case, it should be highlighted that the manufacturing of electrodes for the CV experiments in figure 2b and 2c are different. CVs of figure 2b are performed by dropping cast of the ink onto a polished glassy carbon substrate, while CVs of figure 2c are made by airbrushing technique over a diffusion layer and Toray carbon substrate, as well described in experimental section. Results from Figure 2c reveal that the electrochemical response of 4VP(7)-Pt/C/GDE/T and 4VP(12)-Pt/C/GDE/T in 0.1 M NaOH exhibit still the resolved peaks associated with the adsorption/desorption of hydrogen. Currents normalized by mg of Pt/C catalyst are similar for both electrodes with different 4VP wt.%. However, the CV behavior of figure 2c is dominated by the IR drop from the imposed by the sum of electrical

resistivity of the diffusion layer and Toray carbon substrate. As far as the cohesion of the Pt/CB layer is concerned, we found that a percentage of 4VP below 12 wt. % is critically detrimental for the mechanical stability of the Pt/CB layer, leading to leaching of Pt/CB nanoparticles when the 4VP-Pt/CB/GDE/T electrode is immersed in the alkaline solution. On the other hand, ionomer percentages over 20 wt. % resulted in a complete Pt surface blockage by the 4VP molecules, as shown in Figure 2c, even though the adherence and mechanical properties of the 4VP-Pt/CB/GDE/T improved significantly compared to the other percentages. In this regard, Mamlouk et al. [23] and references therein [22, 41-46] have reviewed the importance of ionomer optimisation on the preparation of catalytic inks, and therefore on the electrocatalytic layers of both cathode and anode electrodes towards hydrogen and direct alcohol alkaline fuel cells. Accordingly, the design of the catalytic ink is crucial to obtain electrodes with improved mechanical, thermal stability, electrocatalytic activity and durability performance. Furthermore, other recent studies reported that the optimum percentage of anionic FAA-3 ionomer that leads to the maximum performance of fuel cell was around 25 wt.% when the electrolyte was 1.0 M NaOH [28]. On the other hand, Leng et al. [47] performed the electrolysis of water using a MEA configuration, in which the anionic AS4 ionomer amount of the catalytic layer in the anode and cathode was 16 wt.%. It should be noted that an excessive amount of ionomer could lead to higher resistance mainly ascribed to the hindering of the reactive diffusion or charge transfer and therefore a subsequent inactivation of the Pt electrocatalyst. On the contrary, a low amount of ionomer can involve high resistance and therefore high IR drops and low OH^- conductivity through the electrocatalytic layer.

Figure 3 depicts the diffractogram of 4VP(12)-Pt/CB/GDE/T surface for the determination of the crystallite size of platinum nanoparticles after cast film formation. The diffraction peaks corresponds to the characteristic face-centered cubic packing structure of Pt [48]. The average crystallite size of Pt was obtained by using the Scherrer equation [49]. Such calculations provided an average crystallite size of Pt of about 3 nm, which is in a good agreement with an average particle size of 2.3 nm of Pt obtained by TEMas determined in a previous work by Lopez Cudero et al. [34]

For 12 wt. % 4VP within the Pt/CB electrocatalytic layer, a highly homogeneous Pt/CB layer was observed in the SEM images of the 4VP(12)-Pt/CB/GDE/T electrode in

Figures 4a and 4c. The surface of the 4VP(12)-Pt/CB cast film shows some cracks, as shown in Figure 4a which were in part attributed to differences in the coefficients of expansion between the cast film and the gas diffusion layer after removal of the ethanolic solution. The EDS mapping of the plane section of electrocatalytic layer (Figure 4b), confirms that the Pt/CB nanoparticles were very uniformly dispersed throughout the diffusion layer/Toray paper without agglomeration. The cross-section of the cathode 4VP(12)-Pt/CB/GDE/T was observed in Figure 4c and 4d, depicting Pt nanoparticles onto the top of the electrocatalytic layer. Figure 4d also reveals that the catalytic metal nanoparticles are mainly coated onto the upper side of the Toray substrate. In this regard, it is of notice that the use of spraying technique for the preparation of the catalytic ink coating successfully minimizes percolation through the Toray paper, leading to homogeneous distribution of the metal catalysts. Figure 4e displays the high resolution SEM images of the surface in 4VP(12)-Pt/CB/GDE/T cathode probing the heterogeneous nature of the electrode surface, though unfortunately no clear distinction of the particle size determination is disclosed from the figure. From the EDS experiments of the 4VP(12)-Pt/CB/GDE/T cathode, it was found wt.% values of 82.66, 4.01, and 13.34 for C, O and Pt, respectively, compared with the calculated wt.% values of 82.39 for C and 17.60 for Pt, respectively,assuming a negligible wt.% value for oxygen present in the Vulcan carbon. Nitrogen presence was negligible in the EDS analysis under the experimental conditions. Hence, calculated and experimental wt. % values are consistently in terms of carbon wt.% content and similar regarding the wt.% of platinum loading. Moreover, EDS analysis provided at. % values of 95.57, 3.47 and 0.95 for C, O and Pt, respectively.

We next revealed the Raman spectrum of the 4VP(12)-Pt/CB/GDE/T electrode, as shown in Figure 5, with the typical band D and G together with the second order bands 2D and D and G. The extra band at ca. 490 cm^{-1} was found to be ascribed to the polymeric binder 4VP. No Raman band was elucidated from the platinum- carbon interaction under our experimental conditions.

3.2 Physicochemical and electrochemical characterisation of the 4VP-Ni/CB/T anode.

Figure 6a depicts the cyclic voltammetric response of the electrochemical activation of Ni surface of the 4VP-Ni/CB/T electrode in 1.0 M NaOH. It is worth noting that 20 wt. % 4VP resulted optimum from mechanical property improvement point of view of the electrocatalytic layer of the Ni/CB. CV behaviour of the 4VP-Ni/CB/T electrode was compared to the same electrode containing a 20 wt. % cationic Nafion ionomer as binder (Figure 6b), i.e. Nafion-Ni/CB/T electrode, characterised in our previous work [24]. The cyclic voltammetric responses demonstrate that both electrodes prepared with different binders exhibited similar voltammetric performance in the absence of PGA. However, it is worth pointing out that the electrochemical responses of 4VP-Ni/CB/T anodes towards the electrooxidation of 0.05 M PGA was slightly higher than when Nafion-Ni/CB/T electrode was used. While the net increase in current associated with the electrooxidation of PGA is 4.0 mA mg^{-1} by using the 4VP ionomer, the Nafion-Ni/CB/T showed only an increment of 2.2 mA mg^{-1} with respect to the current obtained in the absence of alcohol. Moreover, the peak potential for the electrooxidation of PGA using the 4VP-Ni/CB/T electrode was 0.47 V, lower than the value of 0.54 V obtained for the Nafion-Ni/CB/T electrode. It is difficult to ascribe the slight differences in current or oxidation peak potentials noted above, to the effect of the ionomer nature rather than a higher nickel electroactive area or different resistive components indistinguishably observed for both electrodes. Nevertheless, the anionic ionomer is likely the only species in the electrode assembly that allows hydroxide anions transport through the electrocatalytic layer, thereby enhancing the performance of anode electrode [22].

Figure 7 depicts the diffractogram of 4VP-Ni/CB/T surface for the determination of the crystallite size of Ni nanoparticles after cast film formation. A typical diffractogram of Ni with a main peak at near 44º assigned as Ni[111] XRD peak [50]. The crystallite size was calculated as 2.9 nm for the 4VP-Ni/CB which is consistently comparable with an average Ni particle size of 2 nm according to our previous TEM images[24].

The surface and cross sections of the 4VP-Ni/CB/T anode are observed in Figure 8. 4VP-Ni/CB layer displayed a homogeneous coverage of the carbon fibres without any agglomerations. The same results are obtained when Nafion was used as binder [24]. Such a cross section demonstrates that the electrocatalytic layer was deposited onto the

tridimensional electrode surface (Figure 8b and 8d). A deeper observation illustrated in figure 8e through high resolution SEM in the direct determination of metal particle size and distribution of Ni nanoparticles on carbon-support demonstrates the absence of agglomeration of Ni nanoparticles, though yet again particle size was difficult to be identified by this technique. Finally, Raman spectrum shown in Figure 9 exhibited the same patern as that shown in figure 5.

3.3 Polarisation plots using the PEMER configuration.

A polarisation technique was performed for understanding the electrochemical response of the MEA configuration employed when a current or potential are applied under steady conditions. Figure 6 shows the polarisation plots using the PEMER configuration consisting of a 4VP-Ni/CB/T as anode, a 4VP(12)-Pt/CB/GDE/T as cathode and either 4VP/CS:PVA or FAA membranes using a variable concentration of the NaOH solution. Polarisation experiments were performed in the presence of 0.25 M PGA in NaOH solution.

Figure 9a depicts the polarisation plots for different NaOH concentration in the anodic compartment when the FAA commercial AAEM was used. As expected, the cell potential increased as the NaOH concentration decreased. The increase of almost 200 mV at 0.5 A in 0.1 M NaOH was mainly associated with effect of the conductivity of NaOH solution. The use of 0.01 M NaOH resulted in a notable increase in the cell potential up to values of 2 V, where the OH^- consumed during the electrooxidation of PGA come from the membrane itself. Even though the electrooxidation of PGA is viable with a cell potential near 2 V, the chemical stability of the $Ni(OH)_2$ /NiOOH electrocatalyst redox couple is compromised by the pH reduction of the solution during the electrooxidation.

We investigated the influence of the flow rate of the anodic solution through the anode compartment upon the polarisation plots to optimise the cell potential. Within a range of flow rates between 6-20 mL min^{-1} using 1.0 M NaOH solution in the anodic compartment no significant differences in terms of cell potential were observed. The only exception occurred when working at higher currents, where the oxygen evolution was favoured. Under such conditions, the laminar hydrodynamics dominates in the anodic compartment, which turns inefficient or influences very slowly the removal of molecular

oxygen from this compartment. Hence, the orientation of 4VP-NiCB catalytic layer in contact with the membrane or the graphitic column collector was responsible of the increment or reduction of the cell potential, respectively. When the 4VP-Ni/CB electrocatalytic layer was in contact with the graphitic column collector, the cell potential, at least at higher currents, decreased slightly owing likely to an easier evacuation of molecular oxygen bubbles generated from the electrooxidation of water onto the NiOOH electrocatalytic surface. In the case of the influence of air feeding flow rate through the cathodic compartment on the cell potential of the PEMER configuration, no variations of cell potentials were found when feeding air through the 4VP(12)-Pt/CB/GDE/T cathode within a flow rate range between 50 and 200 mL min^{-1}. In view of the above results, we can conclude that a flow rate of 12 mL min^{-1} for the anodic solution, a 50 mL min^{-1} flow rate of air through the cathodic compartment and 1.0 M NaOH solution provided the minimum cell potential for the currents evaluated. Such experimental conditions were chosen to compare the performance of the novel 4VP/CS:PVA membrane with that of the commercial FAA membrane. Figure 9b depicts the polarisation plots for both AAEMs. Within the current range from 0.02 A to 0.1 A, the cell potential resulted higher for the FAA membrane than the 4VP/CS:PVA membrane. This is due to the different activation of the cathodic process, associated with the ORR, which is a function of the type of membrane used. It is worth noting that the membranes display differences regarding water swelling and alcohol permeation properties [26] that affect the performance of the cathode at low currents. Then, after the activation energy for the ORR was reached, the cell potential for the 4VP/CS:PVA membrane increased until values near those for the FAA membrane. On the other hand, the same polarisation plot was also performed using the Nafion-Pt/CB/GDE/T cathode and the Nafion-Ni/CB/T anode deposited on the graphitic columns, with the FAA commercial membrane (results not shown). This configuration provided a cell potential of around 5.0 V for the highest currents tested, demonstrating the detrimental effect of the use of the Nafion ionomer. Moreover, the study of two different PEMER configurations, (i) Nafion-Pt/CB/GDE/T as cathode and 4VP-Ni/CB/T as anode, and (ii) 4VP(12)Pt/CB/GDE/T as cathode and Nafion-Ni/CB/T as anode demonstrated that the highest increase in cell potential was obtained when the Nafion-Pt/CB/GDE/T electrode was used. Hence, it is evident that the use of Nafion as a cationic ionomer for the

preparation of the cathode is disadvantageous in alkaline medium under the experimental conditions of this work, precluding the OH^- transport through the electrocatalytic layer of the Nafion-Pt/CB/ electrode.

3.4. Preparative electrooxidation of propargyl alcohol

We next turned to the preparative electrooxidation of PGA to the corresponding carboxylic acids derivatives (PA and/or PPA) using the PEMER configuration. Preparative electrolysis were performed either using the FAA or the 4VP/CS:PVA membrane. Anodic, cathodic and the overall electrochemical process reactions as well the overall electrochemical process through the NiOOH species formation are displayed in reactions **1-4** as follows,

$$Ni(OH)_2 + OH^- \rightarrow NiOOH + H_2O + e \quad (1)$$

$$NiOOH + CHCCH_2OH + 4OH^- \rightarrow Ni(OH)_2 + CHCCOO^- + 3\,H_2O + 3e \quad (2)$$

$$CHCCOO^- + CHCCH_2OH \rightarrow CHCCH_2OCHCHCOO^- \quad (3)$$

$$O_2 + 2\,H_2O + 4e \rightarrow 4\,OH^- \quad (4)$$

where reactions **2** and **3** denote the formation of PA and Z-PPA, respectively.

Therefore, the primary reaction involves the electrooxidation of PGA to PA throughout the regeneration of NiOOH species to $Ni(OH)_2$ species (reaction 1 and 2) [35, 51, 52]. On the other hand, the electrooxidation of PGA can likely lead to the formation of Z-PPA isomer which proceeds through a hapto-propiolate complex with the NiOOH species on the surface via the triple bond of the alkyne moiety (reaction 3) as described in a tentative mechanism in [14]. The parasite reaction at the anode corresponds to the electrooxidation of water to oxygen. Simultaneously, the reduction of O_2 to OH^- anions as shown in reaction 4 represents the cathodic reaction which is the responsible for the supply OH^- ions necessary (*vide infra)*. Focusing on compartment of anode, it should be pointed out that the electrooxidation of PGA involves the consumption of 5 mole OH^- per mole PGA. With a PGA concentration of 0.250 M within the anodic solution (0.0075 mole of

PGA), the mole of OH^- in 1.0 M NaOH anodic solution (0.03 mole of OH^-) is insufficient to carry out the electrooxidative process of 0.0075 mole PGA to PA under the experimental conditions of the present work, according to reaction **1** and **2**. Thus, the ORR under alkaline conditions occurring in the cathode will supply 4 mole of OH^- (0.0017 mole of OH^- for a theoretical charge of 30 C) per mole molecular oxygen reacted in the cathode. Hence, ORR provides a continuous flux of OH^- to the anodic compartment needed for the electroregeneration of NiOOH species (reaction **1**) and the electrooxidation of PGA (reactions **2** and **3**).

Table 1 displays the conditions established for the electrooxidation of PGA and the obtaining of the final products in terms of current and charge passed. The electrolysis performed using the commercial FAA membrane gave rise to a PGA conversion of 0.74. The use of the 4VP/CS:PVA membrane provided a PGA conversion of 0.77 at a current density of 20 mA cm^{-2}. Z-PPA isomer was the only product obtained from the electrooxidation of PGA as demonstrated by ^1H NMR analysis of the reaction crude obtained after extraction of final anolyte. NMR analysis also demonstrated the absence of oligomerization products in the crude reaction mixture. By assuming that all reacted PGA is converted to Z-PPA, average current efficiencies are 0.31 and 0.33 when using a FAA and 4VP membrane, respectively, after 3 consecutive electrosynthetic reactions for each membrane. Accordingly, there is a fraction of the electrical charge passed which is being used for the side reaction involving the oxidation of water during organic electrosynthesis. Table 1 also shows the space time yield and electrolytic energy consumption.

SEM and XPS analysis were performed for both FAA and 4VP/CS:PVA membranes after electrooxidations and no remarkable difference were observed compared to morphology and surface chemistry results of fresh membranes. Alkaline PEM suffers from a hydroxide/carbonate/bicarbonate equilibrium [53-55]. Such reactions reduce the pH of solution, providing a loss in the alcohol electrooxidation performance. Under our experimental conditions, carbonation fouling was discarded since first, the electrooxidation of PGA led selectively to the formation of the Z-PPA without formation of CO_2, and second, the purity of synthetic air used for the electroreduction of oxygen, discarding the presence of carbonate/bicarbonate in the cathodic side. On the other hand, the use of anion-exchange membrane precludes sodium or potassium cations reaches the cathode where

insoluble sodium or potassium bicarbonate could be formed at room temperature, obstructing the catalytic layer. Moreover, within the time scale of 6 consecutive electrosynthetic reactions, the residual presence of CO_2 into the anodic solution coming from the atmospheric air was practically irrelevant for the performance of the electrooxidation of PGA in terms of conversion and current efficiency. Therefore, the viability of the electrooxidation of PGA in alkaline medium using anion-exchange membrane based on low cost and environmentally friendly polymers as SPE in a PEMER configuration provides the proof of concept necessary to be extrapolated to a vast variety of electrooxidation processes of primary and secondary alcohols.

Finally, the stability of the anode and cathode during the electrooxidation of PGA was proved by consecutive electrolysis using both FAA and 4VP/CS:PVA membranes. Cell potentials were found to be very stable during the electrooxidation of PGA and consequently our results were clearly indicative of a proper performance of all parts of the PEMER configuration. In the case of the mechanical stability of the 4VP-Ni/CB/T and 4VP(12)-Pt/CB/GDE/T electrodes, a more profound investigation by SEM of both electrode surfaces revealed no detachment of the electrocatalytic layer as well as a defect-free surface after repetitive electrolysis.

4. Conclusions

We have demonstrated the viability of the electrooxidation of alcohols in alkaline media either using a commercial anionic alkaline exchange membrane or a newly developed CS:PVA based anion-exchange membrane doped with 4VP ionomer in a PEMER configuration. A 12 wt. % 4VP anionic ionomer concentration with respect to Pt/CB electrocatalyst was optimum in terms of particle cohesion and electrocatalytic response measured by the adsorption/desorption of hydrogen, and facilitated an excellent attachment to the carbonaceous substrate (either gas diffusion layer or Toray paper substrates). Moreover a 20 wt.% of 4VP with respect to Ni/CB electrocatalyst was the optimum towards mechanical and cohesion of the cast film on the Toray paper. XRD measurements provided valuable outcome into the crystallographic properties of the Pt/CB and Ni/CB electrocatalysts in the presence of the anionic ionomer binder after spraying coating. The crystal structure of Pt was determined by XRD and found to be face centered

cubic. The average crystallite size of Pt nanoparticles was calculated from X-ray diffraction peak widths and found to be 3 nm, which is in a good agreement with an average particle size of 2.3 nm according to previous TEM measurements. Crystallite size of Ni nanoparticles was found to be 2.9 nm close to our average particle size of 2 nm obtained by TEM. High resolution SEM .images displayed no formation of large agglomerated particles for any of Pt/CB or Ni/CB electrocatalysts. Raman spectra for both electrocatalysts revealed the typical D and G bands along with the second order bands. The Raman shift was clearly observed for the 4VP anionic ionomer circa 490 cm^{-1}, and no observation of either Pt-C or Ni-C interactions.

Polarisation curves confirmed that the cell potentials of the PEMER configuration when using the 4VP/CS:PVA membrane exhibited similar values to those ones for FAA commercial membrane for currents between 0.1 and 0.5 A. The main product obtained from the electrooxidation of PGA in our PEMER configuration under the experimental conditions of a current density of 20 mA cm^{-2} and a Ni loading of 0.1 mg cm^{-2} was Z isomers of 3-(2-propynoxy)-2-propenoic acid, with a fractional conversion of 0.74-0.77 for 2895 C of charge passed and with current efficiency and specific electrolytic energy consumption practically equal than those for FAA membrane. Furthermore, the performance of the new 4VP/CS:PVA membrane was comparable to that of the FAA commercial membrane in terms of alkaline stability.Last but not the least, the performance and mechanical integrity of both 4VP(12)-Pt/CB/GDE/T and 4VP-Ni/CB/T electrodes were stable at least with repetitive PGA electrooxidations.

Acknowledgements

This work has been funded by the Spanish MINECO through grants CTQ2010-20347, at the University of Alicante, and CTQ2012-31229 and RYC2011-08550, at the University of Cantabria. L.G.C. for her PhD fellowship BES-2011-045147 at the University of Alicante and the EEBB-14-09094 mobility grant to go on a research stay to the University of Cantabria. The authors gratefully thank Dr. José Solla Gullón for his advice on the synthesis of platinum nanoparticles, from the Institute of Electrochemistry of University of Alicante.

References

[1] J. Yoshida, K. Kataoka, R. Horcajada, A. Nagaki, Modern strategies in electroorganic synthesis, Chem. Rev. 108 (2008) 2265.
[2] F.F. Rivera, C.P. de León, J.L. Nava, F.C. Walsh, The filter-press FM01-LC laboratory flow reactor and its applications, Electrochim. Acta 163 (2015) 338.
[3] P. Millet, F. Andolfatto, R. Durand, Design and performance of a solid polymer electrolyte water electrolyzer, Int. J. Hydrogen Energy 21 (1996) 87.
[4] A. Brouzgou, A. Podias, P. Tsiakaras, PEMFCs and AEMFCs directly fed with ethanol: A current status comparative review, J. Appl. Electrochem. 43 (2013) 119.
[5] V. Montiel, A. Sáez, E. Expósito, V. García-García, A. Aldaz, Use of MEA technology in the synthesis of pharmaceutical compounds: The electrosynthesis of N-acetyl-l-cysteine, Electrochem. Commun, 12 (2010) 118.
[6] A. Sáez, V. García-García, J. Solla-Gullón, A. Aldaz, V. Montiel, Electrochemical synthesis at pre-pilot scale of 1-phenylethanol by cathodic reduction of acetophenone using a solid polymer electrolyte, Electrochem. Commun, 34 (2013) 316.
[7] A. Saez, V. Garcia-Garcia, J. Solla-Gullon, A. Aldaz, V. Montiel, Electrocatalytic hydrogenation of acetophenone using a Polymer Electrolyte Membrane Electrochemical Reactor, Electrochim. Acta 91 (2013) 69.
[8] Z. Ogumi, K. Nishio, S. Yoshizawa, Application of the spe method to organic electrochemistry—II. Electrochemical hydrogenation of olefinic double bonds, Electrochim. Acta 26 (1981) 1779.
[9] Z. Ogumi, M. Inaba, S.-i. Ohashi, M. Uchida, Z.-i. Takehara, Application of the SPE method to organic electrochemistry—VII. The reduction of nitrobenzene on a modified Pt-nafion, Electrochim. Acta, 33 (1988) 365.
[10] Z. Ogumi, S. Ohashi, Z. Takehara, Application of the SPE method to organic electrochemistry—VI. Oxidation of cyclohexanol to cyclohexanone on Pt-SPE in the presence of iodine and iodide, Electrochim. Acta 30 (1985) 121.
[11] Z. Ogumi, K. Inatomi, J.T. Hinatsu, Z.-i. Takehara, Application of the SPE method to organic electrochemistry—XIII. Oxidation of geraniol on Mn,Pt-Nafion, Electrochim.a Acta 37 (1992) 1295.
[12] A.J. Motheo, G. Tremiliosi, E.R. Gonzalez, K.B. Kokoh, J.M. Leger, C. Lamy, Electrooxidation of benzyl alcohol and benzaldehyde on a nickel oxy-hydroxide electrode in a filter-press type cell, J. Appl. Electrochem. 36 (2006) 1035.
[13] L. Roquet, E.M. Belgsir, J.M. Léger, C. Lamy, Electrocatalytic oxidation of propargyl alcohol at platinum electrodes in acid medium: A kinetic study, Electrochim. Acta 41 (1996) 1533.
[14] L. García-Cruz, J. Iniesta, T. Thiemann, V. Montiel, Surprising electrooxidation of propargyl alcohol to (Z)-3-(2-propynoxy)-2-propenoic acid at a NiOOH electrode in alkaline medium, Electrochem. Commun. 22 (2012) 200.
[15] G. Merle, M. Wessling, K. Nijmeijer, Anion exchange membranes for alkaline fuel cells: A review, J. Membr. Sci. 377 (2011) 1.
[16] Y.J. Wang, J. Qiao, R. Baker, J. Zhang, Alkaline polymer electrolyte membranes for fuel cell applications, Chem. Soc. Rev. 42 (2013) 5768.
[17] E. Antolini, E.R. Gonzalez, Alkaline direct alcohol fuel cells, J. Power Sources 195 (2010) 3431.

[18] J. Ma, Y. Sahai, Chitosan biopolymer for fuel cell applications, Carbohydr Polym, 92 (2013) 955.
[19] J. Maiti, N. Kakati, S.H. Lee, S.H. Jee, B. Viswanathan, Y.S. Yoon, Where do poly(vinyl alcohol) based membranes stand in relation to Nafion® for direct methanol fuel cell applications?, J. Power Sources 216 (2012) 48.
[20] L. Garcia-Cruz, C. Casado-Coterillo, J. Iniesta, V. Montiel, A. Irabien, Preparation and characterization of novel chitosan-based mixed matrix membranes resistant in alkaline media, J. Appl. Polym. Sci. 132 (2015).
[21] R.K. Nagarale, G.S. Gohil, V.K. Shahi, R. Rangarajan, Preparation of organic-inorganic composite anion-exchange membranes via aqueous dispersion polymerization and their characterization, J. Colloid Interface Sci. 287 (2005) 198.
[22] Y.S. Li, T.S. Zhao, Z.X. Liang, Effect of polymer binders in anode catalyst layer on performance of alkaline direct ethanol fuel cells, J. Power Sources 190 (2009) 223.
[23] M. Mamlouk, K. Scott, J.A. Horsfall, C. Williams, The effect of electrode parameters on the performance of anion exchange polymer membrane fuel cells, Int. J. Hydrogen Energy 36 (2011) 7191.
[24] L. Garcia-Cruz, A. Saez, C.O. Ania, J. Solla-Gullon, T. Thiemann, J. Iniesta, V. Montiel, Electrocatalytic activity of Ni-doped nanoporous carbons in the electrooxidation of propargyl alcohol, Carbon 73 (2014) 291.
[25] I. Epelboin, M. Keddam, H. Takenouti, Use of impedance measurements for the determination of the instant rate of metal corrosion, J. Appl. Electrochem. 2 (1972) 71.
[26] L. García-Cruz, C. Casado-Coterillo, J. Iniesta, V. Montiel, Á. Irabien, Chitosan:poly (vinyl) alcohol composite alkaline membrane incorporating organic ionomers and layered silicate materials into a PEM electrochemical reactor, J. Membr. Sci. 498 (2016) 395.
[27] K. Matsuoka, Y. Iriyama, T. Abe, M. Matsuoka, Z. Ogumi, Alkaline direct alcohol fuel cells using an anion exchange membrane, J. Power Sources 150 (2005) 27.
[28] M. Carmo, G. Doubek, R.C. Sekol, M. Linardi, A.D. Taylor, Development and electrochemical studies of membrane electrode assemblies for polymer electrolyte alkaline fuel cells using FAA membrane and ionomer, J. Power Sources 230 (2013) 169.
[29] A. Santasalo-Aarnio, P. Peljo, E. Aspberg, K. Kontturi, T. Kallio, Methanol, Ethanol and Iso-propanol Performance in Alkaline Direct Alcohol Fuel Cell (ADAFC), Polymer Electrolyte Fuel Cells 10, Pts 1 and 2, 33 (2010) 1701-1714.
[30] A. Santasalo-Aarnio, S. Hietala, T. Rauhala, T. Kallio, In and ex situ characterization of an anion-exchange membrane for alkaline direct methanol fuel cell (ADMFC), J. Power Sources 196 (2011) 6153..
[31] J.Iniesta. Vicente Montiel, Leticia García-Cruz, Thies Thiemann, Procedimiento estereoselectivo para la síntesis electroquímica del ácido 3-(2-propinoxi)-2-propenoico, WO2013167779 A1, 2013.
[32] W.Z. Li, W.J. Zhou, H.Q. Li, Z.H. Zhou, B. Zhou, G.Q. Sun, Q. Xin, Nano-stuctured Pt-Fe/C as cathode catalyst in direct methanol fuel cell, Electrochim. Acta 49 (2004) 1045.
[33] J. Prabhuram, T.S. Zhao, C.W. Wong, J.W. Guo, Synthesis and physical/electrochemical characterization of Pt/C nanocatalyst for polymer electrolyte fuel cells, J. Power Sources 134 (2004) 1.
[34] A. Lopez-Cudero, J. Solla-Gullon, E. Herrero, A. Aldaz, J.M. Feliu, CO electrooxidation on carbon supported platinum nanoparticles: Effect of aggregation, J. Electroanal. Chem. 644 (2010) 117.

[35] Q. Yi, J. Zhang, W. Huang, X. Liu, Electrocatalytic oxidation of cyclohexanol on a nickel oxyhydroxide modified nickel electrode in alkaline solutions, Catal. Commun. 8 (2007) 1017.
[36] M.A. Abdel Rahim, R.M. Abdel Hameed, M.W. Khalil, Nickel as a catalyst for the electro-oxidation of methanol in alkaline medium, J. Power Sources, 134 (2004) 160.
[37] C.M. Sanchez-Sanchez, E. Exposito, J. Solla-Gullon, V. Garcia-Garcia, V. Montiel, A. Aldaz, Calculation of the characteristic performance indicators in an electrochemical process, J. Chem. Educ. 80 (2003) 529.
[38] F.C. Walsh, A First Course in Electrochemical Engineering, Electrochemical Consultancy, 1993.
[39] F.J. Vidal-Iglesias, R.M. Arán-Ais, J. Solla-Gullón, E. Herrero, J.M. Feliu, Electrochemical characterization of shape-controlled Pt nanoparticles in different supporting electrolytes, ACS Catalysis 2 (2012) 901.
[40] M.J.S. Farias, F.J. Vidal-Iglesias, J. Solla-Gullón, E. Herrero, J.M. Feliu, On the behavior of CO oxidation on shape-controlled Pt nanoparticles in alkaline medium, J. Electroanal. Chem. 716 (2014) 16.
[41] M. Mamlouk, X. Wang, K. Scott, J.A. Horsfall, C. Williams, Characterization and application of anion exchange polymer membranes with non-platinum group metals for fuel cells, Proc. Inst. Mech. Eng. Part A J. Power Eng. 225 (2011) 152.
[42] J. Pan, S. Lu, Y. Li, A. Huang, L. Zhuang, J. Lu, High-Performance Alkaline Polymer Electrolyte for Fuel Cell Applications, Adv. Funct. Mater. 20 (2010) 312.
[43] E.E. Switzer, T.S. Olson, A.K. Datye, P. Atanassov, M.R. Hibbs, C. Fujimoto, C.J. Cornelius, Novel KOH-free anion-exchange membrane fuel cell: Performance comparison of alternative anion-exchange ionomers in catalyst ink, Electrochim. Acta 55 (2010) 3404.
[44] M. Piana, M. Boccia, A. Filpi, E. Flammia, H.A. Miller, M. Orsini, F. Salusti, S. Santiccioli, F. Ciardelli, A. Pucci, H2/air alkaline membrane fuel cell performance and durability, using novel ionomer and non-platinum group metal cathode catalyst, J. Power Sources 195 (2010) 5875.
[45] H. Bunazawa, Y. Yamazaki, Influence of anion ionomer content and silver cathode catalyst on the performance of alkaline membrane electrode assemblies (MEAs) for direct methanol fuel cells (DMFCs), J. Power Sources 182 (2008) 48.
[46] F. Bidault, D.J.L. Brett, P.H. Middleton, N.P. Brandon, Review of gas diffusion cathodes for alkaline fuel cells, J. Power Sources 187 (2009) 39.
[47] Y. Leng, G. Chen, A.J. Mendoza, T.B. Tighe, M.A. Hickner, C.-Y. Wang, Solid-State Water Electrolysis with an Alkaline Membrane, J. Am. Chem. Soc., 134 (2012) 9054-9057.
[48] T. Hyde, Crystallite Size Analysis of Supported Platinum Catalysts by XRD, Platinum Met. Rev. 52 (2008) 129.
[49] E.F. Kaelble, Handbook of X-rays: for diffraction, emission, absorption, and microscopy, McGraw-Hill, 1967.
[50] J.T. Richardson, R. Scates, M.V. Twigg, X-ray diffraction study of nickel oxide reduction by hydrogen, Appl. Catal. A 246 (2003) 137.
[51] D.K. Bediako, B. Lassalle-Kaiser, Y. Surendranath, J. Yano, V.K. Yachandra, D.G. Nocera, Structure-Activity Correlations in a Nickel-Borate Oxygen Evolution Catalyst, J. Am. Chem. Soc., 134 (2012) 6801.
[52] M.A.A. Rahim, R.M.A. Hameed, M.W. Khalil, Nickel as a catalyst for the electro-oxidation of methanol in alkaline medium, J. Power Sources 134 (2004) 160.

[53] Y. Leng, L. Wang, M.A. Hickner, C.-Y. Wang, Alkaline membrane fuel cells with in-situ cross-linked ionomers, Electrochim. Acta 152 (2015) 93.
[54] J.R. Varcoe, P. Atanassov, D.R. Dekel, A.M. Herring, M.A. Hickner, P.A. Kohl, A.R. Kucernak, W.E. Mustain, K. Nijmeijer, K. Scott, T.W. Xu, L. Zhuang, Anion-exchange membranes in electrochemical energy systems, Energy Environ. Sci. 7 (2014) 3135.
[55] Y.J. Wang, J.L. Qiao, R. Baker, J.J. Zhang, Alkaline polymer electrolyte membranes for fuel cell applications, Chem. Soc. Rev. 42 (2013) 5768.

Figures and Table captions

Figure 1. Scheme of a homemade PEMER configuration used for the electro-oxidation of PGA.

Figure 2. (a) Cyclic voltammetry of the electrochemical response of PtNPs in the absence of 4VP cast onto a GC electrode. (b) Cyclic voltammetry of the electrochemical response of PtNPs with different content of 4VP cast onto a GC electrode. (c) Cyclic voltammetry of the electrochemical response of 4VP(z)-Pt/CB/GDE/T electrodes. 0.1 M NaOH. Scan rate 10 mV s^{-1}. Fifth scan recorded.

Figure 3. Diffractogram of Pt-based electrocatalyst from the 4VP(12)-Pt/CB/GDE/T cathode.

Figure 4. SEM images of (a) plane section of the 4VP(12)-Pt/CB/GDE/T, (b) Pt mapping of the plane section of the 4VP(12)-Pt/CB/GDE/T, (c) cross section of the 4VP(12)-Pt/CB/GDE/T, (c inset) magnification of cross section of the 4VP(12)-Pt/CB/GDE/T, and (d) Pt mapping of cross section of the 4VP(12)-Pt/CB/GDE/T.

Figure 5. Raman spectrum of the 4VP(12)-Pt/CB/GDE/T electrode. * denotes the Raman shift for the 4VP anionic ionomer.

Figure 6. Cyclic voltammetry of the electrochemical response of Ni/CB/T electrode with 20 wt.% of 4VP (a), and Ni/CB/T electrode with 20 wt.% of Nafion (b). 1.0 M NaOH (solid line) and in the presence of 0.05 M PGA (dashed line). Scan rate = 10 mV s^{-1}. Third scan recorded. Geometric area: 0.35 cm^2.

Figure 7. Diffractogram of Ni-based electrocatalyst from the Ni/CB/T anode.

Figure 8. SEM images of Ni/CB/T anode with 20 wt.% of anionic ionomer 4VP of plane section (a) and cross section (b). Ni mapping of plane section (c) and cross section (d).

Figure 9. (a) Polarisation plots using a PEMER configuration and the FAA membrane with different NaOH concentration. The range of current is set between 0.020 A and 0.500 A. (b) Polarisation plots using a PEMER configuration as a function of the membrane. 1.0 M NaOH plus 0.250 M PGA. The range of current is between 0.020 A and 0.500 A. Flow rate of 12 mL min^{-1} for the anodic compartment, and 50 mL $min^{-1}$for the synthetic air through the cathodic compartment.

Scheme 1. Structure of the methyl chloride quaternary cross-linked poly (4-vinylpyridine) ion exchange ionomer resin.

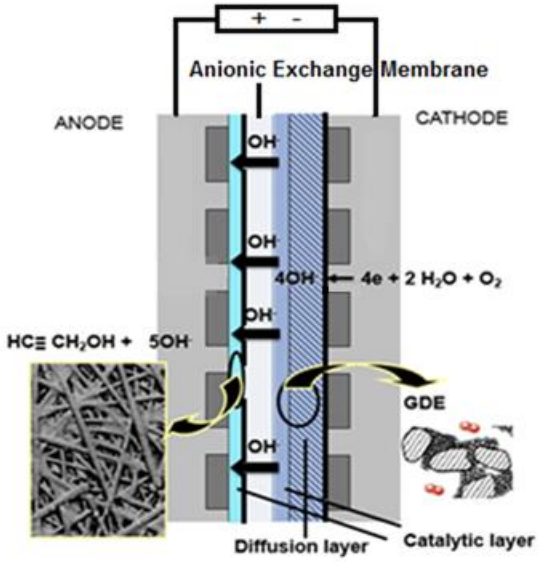

Figure 1.

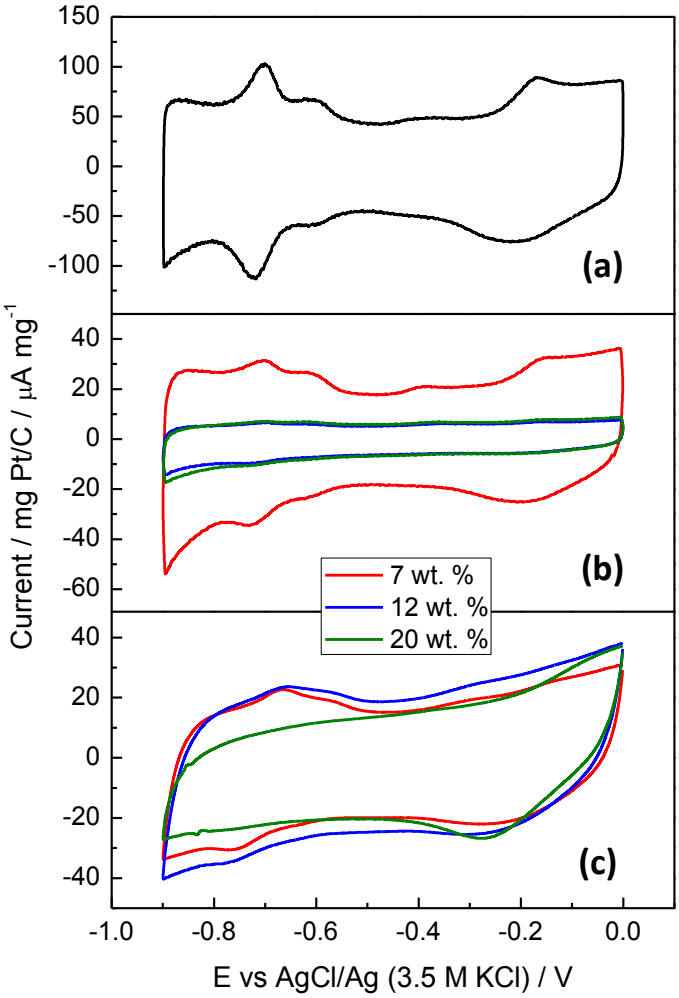

Figure 2.

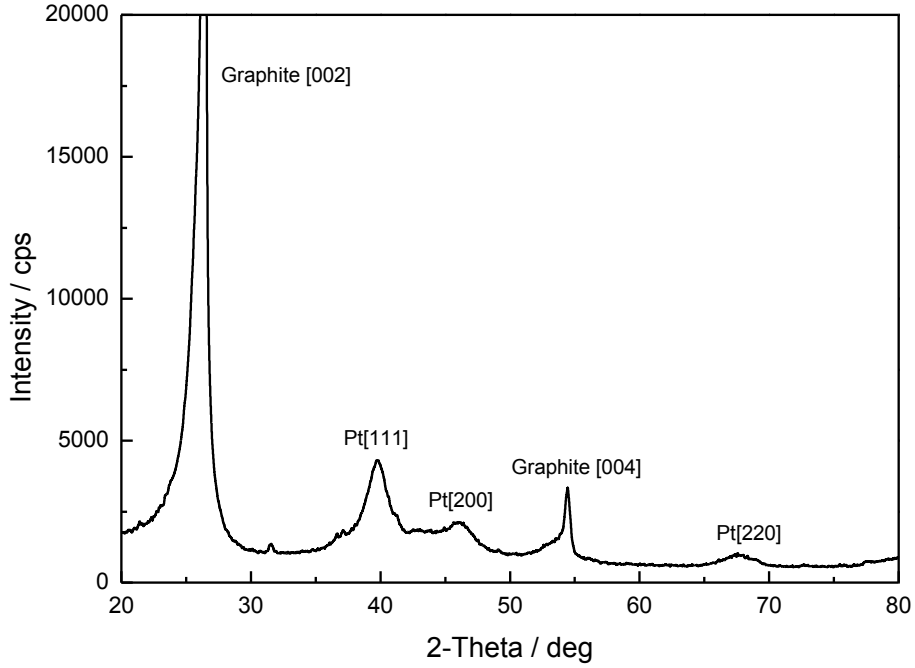

Figure 3.

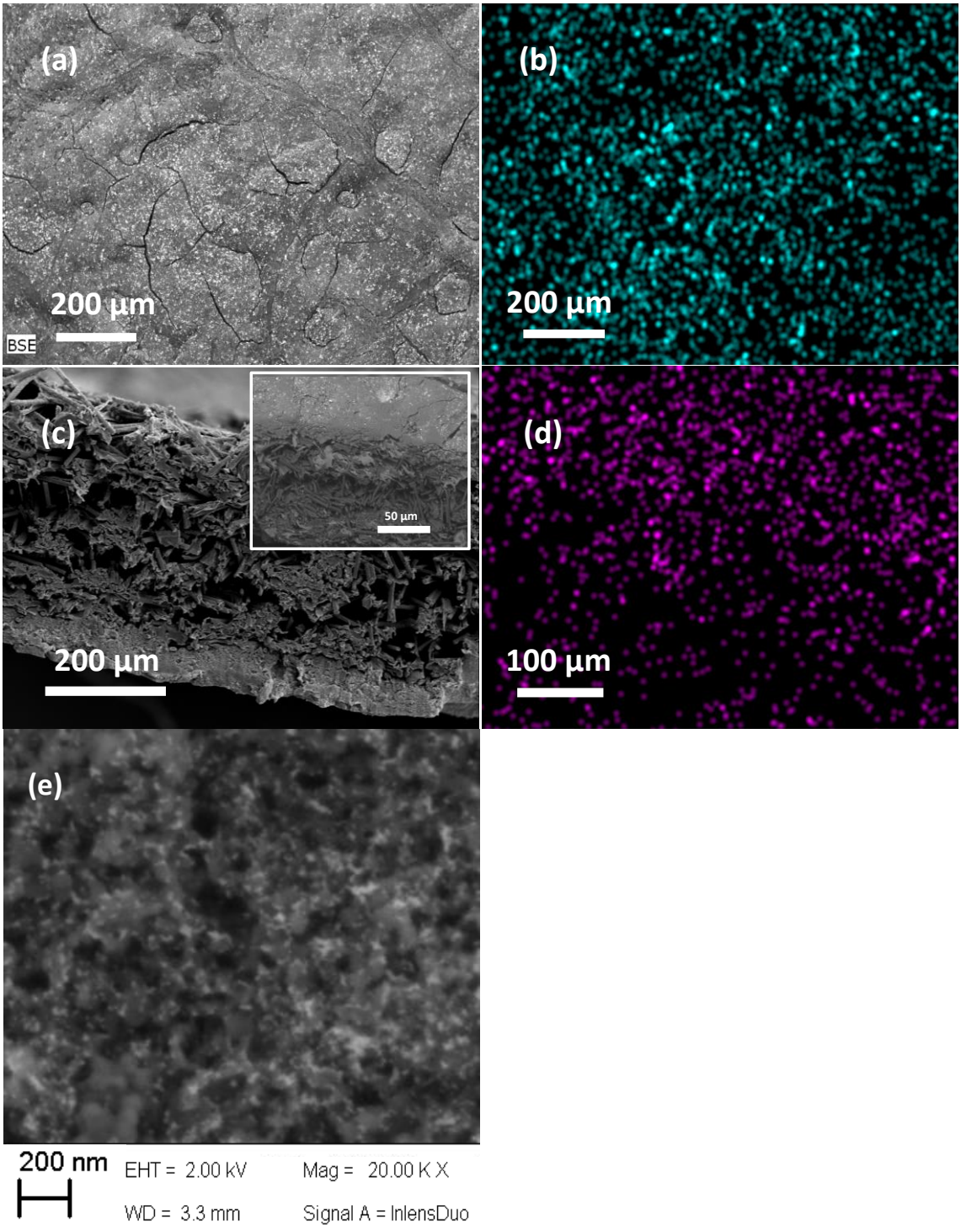

Figure 4.

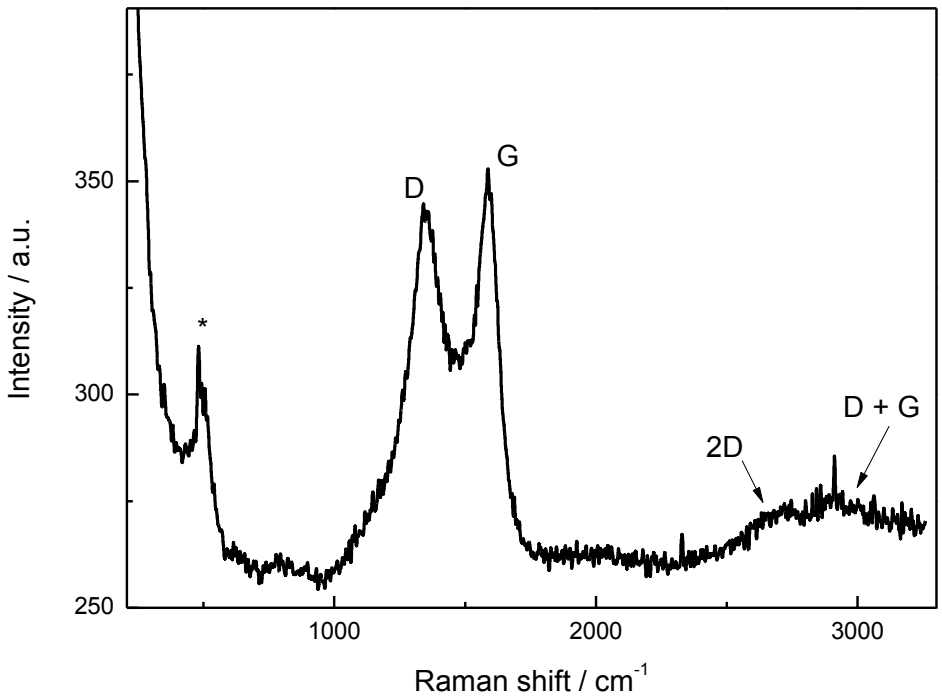

Figure 5.

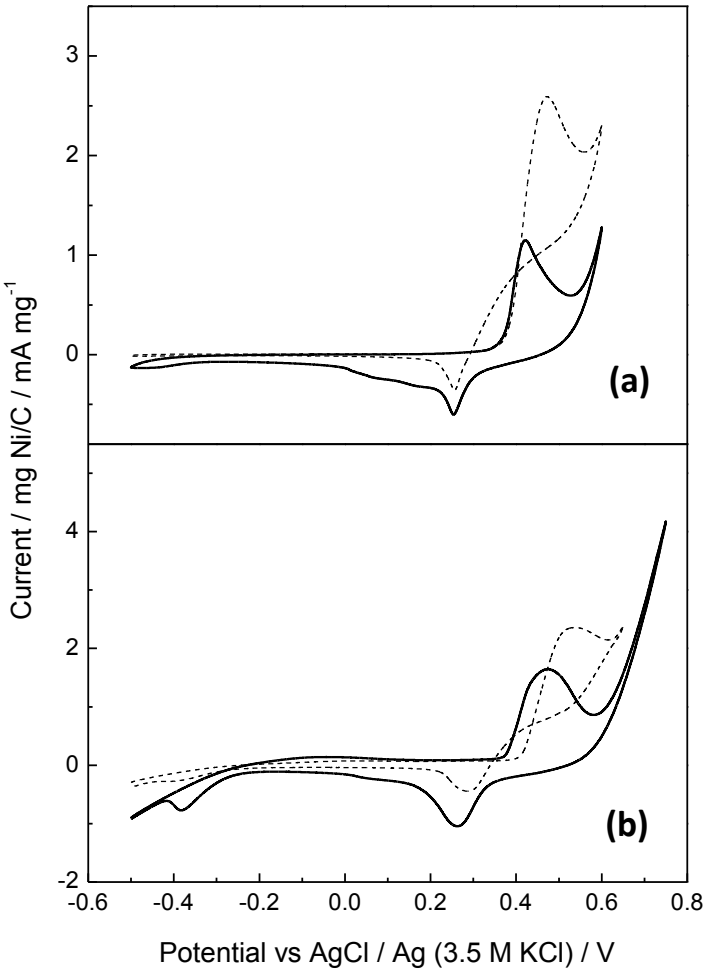

Figure 6.

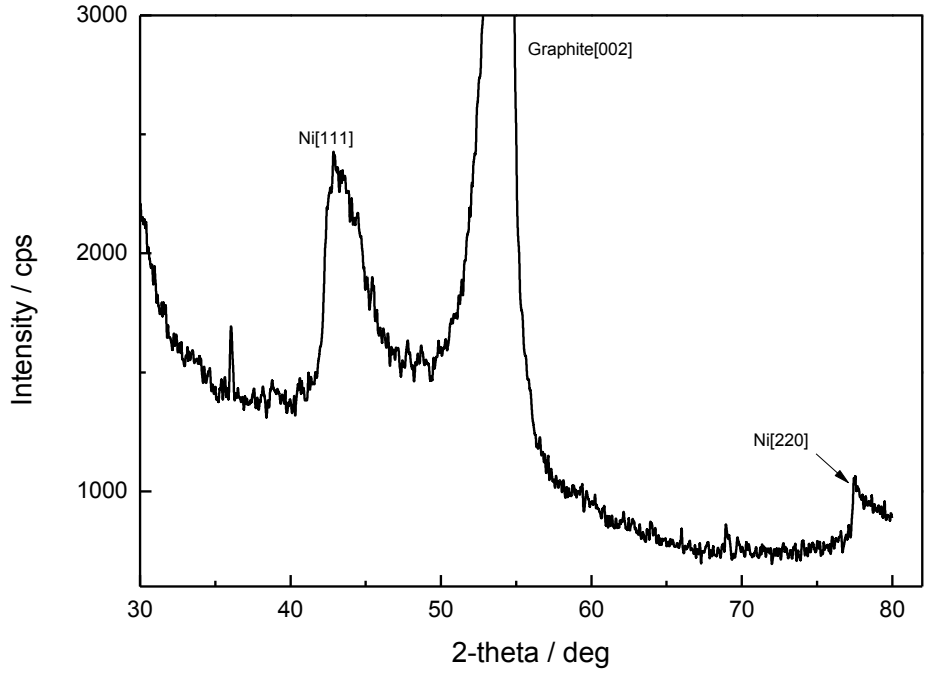

Figure 7.

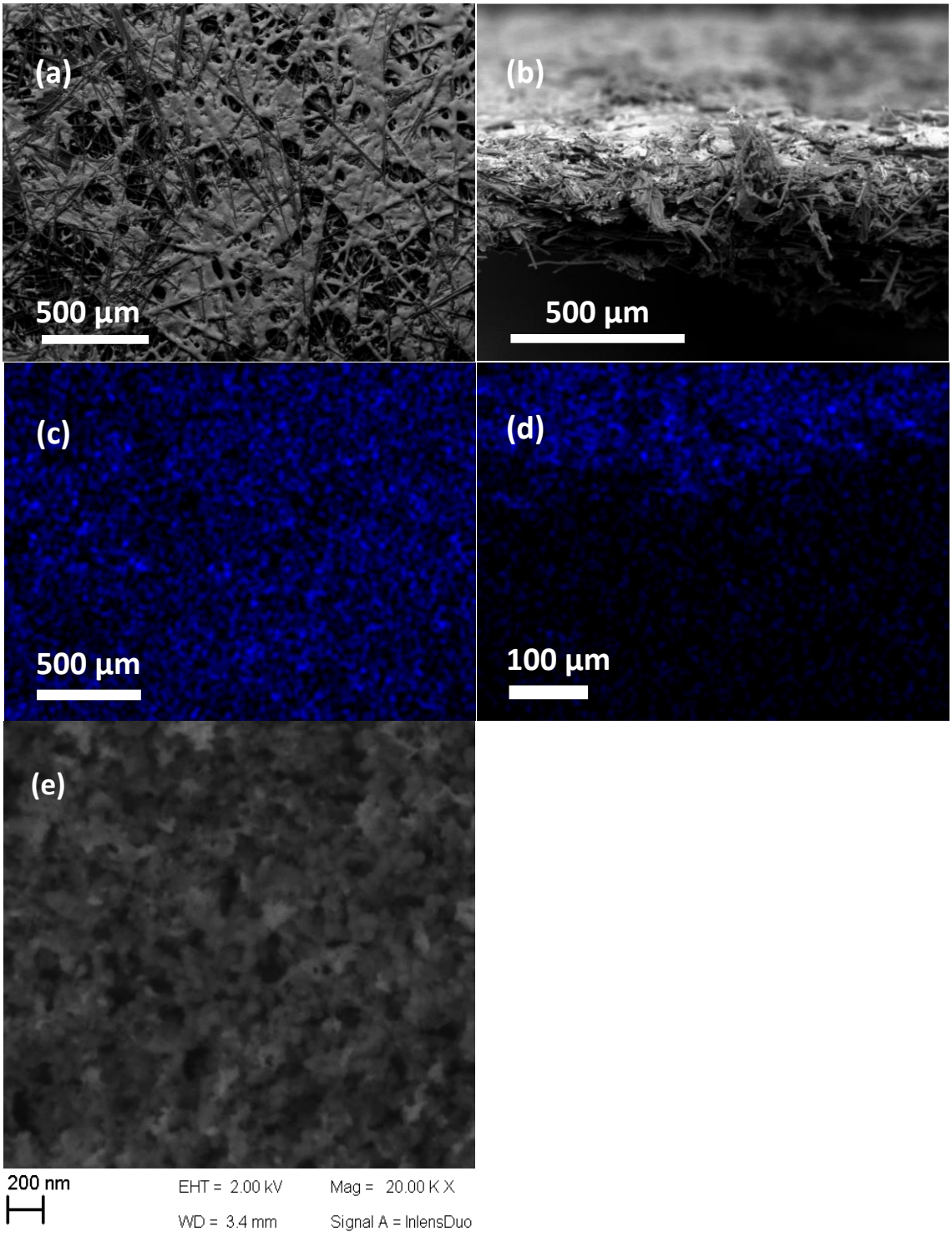

Figure 8.

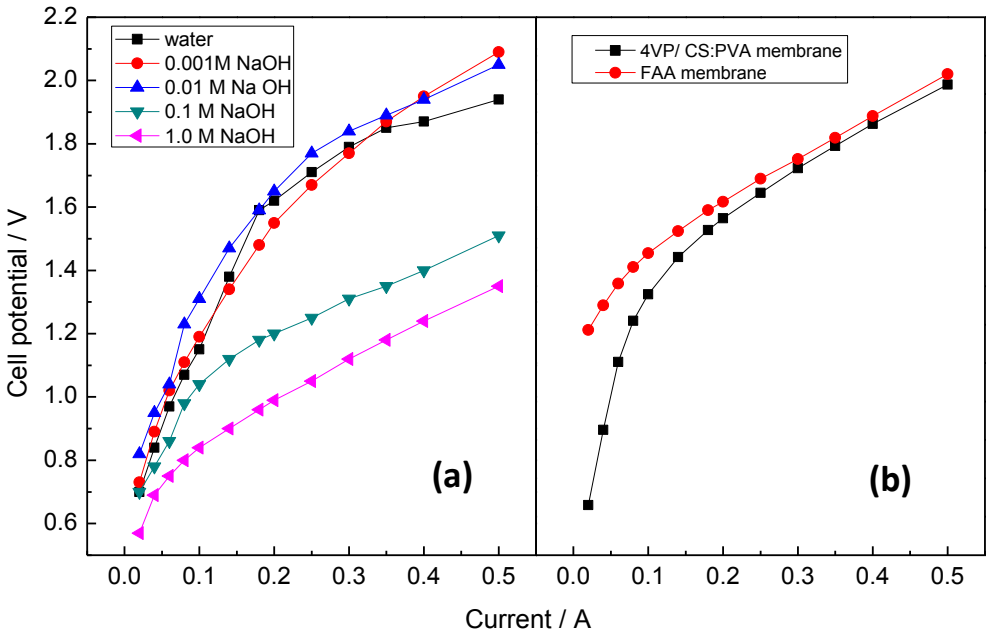

Figure 9.

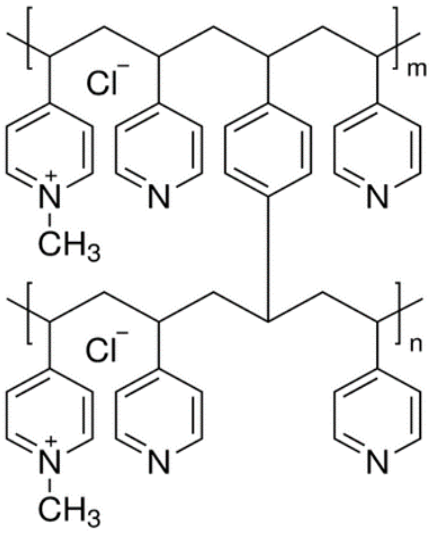

Scheme 1.

Table 1. Experimental conditions and results obtained from the preparative electrooxidation of PGA using both FAA and 4VP/CS:PVA membranes.

	Initial amount PGA / mole	**Anolyte flow rate / mL min^{-1}**		**Catholyte flow rate / mL min^{-1}**	**j / mA cm^{-2}**	**Tempetature / ºC**	**Final pH**
ELECTROLYSIS CONDITIONS	0.0075 (0.25 M)	12		50	20	25 ± 1	14
	Membrane	**PGA conversion $\chi_{PGAconversion}$**	**Current efficiency, ϕ_P**	**Products**	***Space time yield / Kg m^{-3} day^{-1}**	***Specific electrolytic energy consumption / kWh kg^{-1}**	**Average Cell potential/ V**
RESULTS	FAA	0.74	0.31	Z-PPA	14574	3.32	1.21 ± 0.01
	4VP/CS:PVA	0.77	0.33	Z-PPA	15514	3.22	1.25 ± 0.04

*Specific electrolytic energy consumption and space time yield were calculated according to references [37] and [38], respectively, where the specific volume V_e has been considered as geometric volume, 25 cm^2 x thickness of electrode.